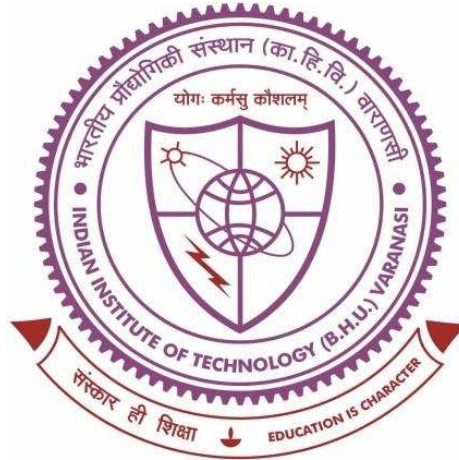


STUDIES ON TRIBOLOGICAL PERFORMANCE OF LASER TEXTURED BEARING STEEL



Thesis submitted in partial fulfillment for the
Award of Degree

Doctor of Philosophy

By

MANISH KUMAR

DEPARTMENT OF MECHANICAL ENGINEERING
INDIAN INSTITUTE OF TECHNOLOGY
(BANARAS HINDU UNIVERSITY)
VARANASI - 221005

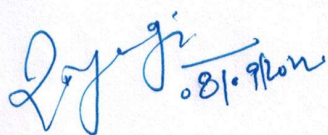
Roll No. 14131002

2022

CERTIFICATE

It is certified that the work contained in the thesis titled "***STUDIES ON TRIBOLOGICAL PERFORMANCE OF LASER TEXTURED BEARING STEEL***" by "***MANISH KUMAR***" has been carried out under our supervision and that this work has not been submitted elsewhere for a degree.

It is further certified that the student has fulfilled all the requirements of Comprehensive Examination, Candidacy, and SOTA for the award of Ph.D. Degree.

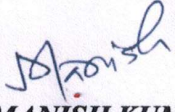


Supervisor
(Prof. Rajnesh Tyagi)
IIT (BHU), Varanasi
INDIA

DECLARATION BY THE CANDIDATE

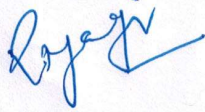
I, "**MANISH KUMAR**", certify that the work embodied in this thesis is my own bonafide work and carried out by me under the supervision of "**Prof. RAJNESH TYAGI**" from "**JULY 2014**" to "**SEPTEMBER 2022**", at the "**DEPARTMENT OF MECHANICAL ENGINEERING**", Indian Institute of Technology (BHU), Varanasi, India and "**DEPARTMENT OF MECHANICAL ENGINEERING**". The matter embodied in this thesis has not been submitted for the award of any other degree/diploma. I declare that I have faithfully acknowledged and given credits to the research workers wherever their works have been cited in my work in this thesis. I further declare that I have not wilfully copied any other's work, paragraphs, text, data, results, *etc.*, reported in journals, books, magazines, reports, dissertations, theses, *etc.*, or available at websites and have not included them in this thesis and have not cited as my own work.

Date: 8th Sept 2022
Place: Varanasi


(**MANISH KUMAR**)

CERTIFICATE BY THE SUPERVISORS

It is certified that the above statement made by the student is correct to the best of our knowledge.



Supervisor
(Prof. Rajnesh Tyagi)
IIT (BHU), Varanasi
INDIA



Signature of Head of Department

विभागाध्यक्ष / HEAD

मक अभियान्त्रिकी विभाग / Deptt. of Mechanical Engg.
भारतीय प्रौद्योगिकी संस्थान / Indian Institute of Technology
(का०हि०वि० / B.H.U.)

वाराणसी-221005 / Varanasi-221005

COPYRIGHT TRANSFER CERTIFICATE

Title of the Thesis: Studies on Tribological Performance of Laser Textured Bearing Steel

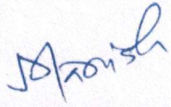
Name of the Student: Manish Kumar

Copyright Transfer

The undersigned hereby assigns to the Indian Institute of Technology (Banaras Hindu University), Varanasi all rights under copyright that may exist in and for the above thesis submitted for the award of the **Doctor of Philosophy**.

Date: 08/09/2022

Place: Varanasi


(Manish Kumar)

Note: However, the author may reproduce or authorize others to reproduce material extracted verbatim from the thesis or derivative of the thesis for the author's personal use provided that the source and the Institute's copyright notice are indicated.

ACKNOWLEDGEMENT

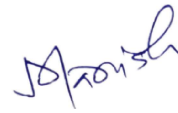
The author is pleased to express his sincere thanks and gratitude beyond words to his supervisor Prof. Rajnesh Tyagi for his consistent help, encouragement and valuable discussions during the entire period of his research work. The author would not have been able to complete the thesis without their utmost involvement and invaluable efforts. They motivated the author to pursue research problems and the need for persistent effort to accomplish the goal. The author is truly indebted to them.

Besides supervisors, the author would like to thank his RPEC members, Prof. Rajesh Kumar and Prof. Sunil Mohan, for their insightful comments and encouragement. The author acknowledges his deep sense of gratitude to the current and former Heads of the Department of Mechanical Engineering for providing all the research facilities to accomplish his research in the Department successfully. The author has an immense sense of gratitude to all the faculty members of the Department of Mechanical Engineering, IIT (BHU), Varanasi, for their cooperation and inspiration.

The author is grateful to all his friends Dr. Rohit Kumar Singh Gautam, Dr. Hemant Nautiyal, Dr. Sudesh Singh, Mr. Praveen Kumar Singh, Mr. Satish Upadhyaya, Mr. Dheeraj Kumar Singh, Mr. Shivanshu Shekhar, Mr. Sushil Yadav, Mr. Rabindra Prasad, Mr. Ashish Pareta, Mr. Akash Awale, Mr. Ashwani Ranjan, Mr. Sanjay Gupta, Ms. Pooja Verma, Mr. Nitish Mahto, Smt. Smita Gupta, Mr. Adarsh Kumar and seniors especially Dr. Pushkar Jha, Dr. Avinash Ravi Raja, Dr. Manvendra Singh, and Dr. Prashant Kumar for their constant encouragement, making joyful and memorable life being with him in moments of happiness and difficulties at IIT (BHU), Varanasi. The author is also thankful to all the lab and office staff of the Department, especially Mr. Vijay Pratap Srivastava (CAM lab).

The author would also like to express his immense gratitude to his parents Smt. Manju Gupta and Shri Gopal Prasad Gupta, brother Praveen Kumar, wife Madhawi Kumari, daughter Ms. Deepanshi and sisters Madhu Gupta, Anju Gupta, Mamta Gupta for their unconditional support and encouragement to pursue his interest. The author also wishes to thank all those who have helped in any manner during the course of his research work.

At last thanks to the almighty God who has given the author spiritual support and courage to carry out this work.

A handwritten signature in blue ink, appearing to read 'Manish' with a stylized flourish.

(MANISH KUMAR)

TABLE OF CONTENTS

<i>CONTENTS</i>	Page No.
<i>LIST OF FIGURES</i>	xi
<i>LIST OF TABLES</i>	xviii
<i>LIST OF ABBREVIATIONS/SYMBOLS</i>	xix
<i>PREFACE</i>	xxi
Chapter 1 INTRODUCTION	1
Chapter 2 REVIEW OF LITERATURE	8
2.1 SURFACE INTERACTIONS AND WEAR	9
2.1.1 SURFACE CONTACTS	11
2.1.2 FRICTION	12
2.1.3 WEAR	14
2.1.3.1 TYPES OF WEAR	15
2.2 MINIMISATION OF FRICTION AND WEAR	16
2.3 LUBRICATION	18
2.3.1 REGIMES OF LUBRICATION	20
2.4 SURFACE TEXTURING	24
2.4.1 DESIGN PARAMETERS	26
2.4.1.1 DIMPLE SHAPE	26
2.4.1.2 DIMPLE DEPTH	27
2.4.1.3 DIMPLE DENSITY	28
2.4.1.4 ARRAY OF DIMPLES	29
2.4.2 SURFACE TEXTURING TECHNIQUES	30

2.4.2.1	LASER SURFACE TEXTURING	31
2.4.2.1.1	LASER-INDUCED ABLATION	32
2.4.2.1.2	DIRECT LASER INTERFERENCE PATTERNING (DLIP)	32
2.4.2.1.3	LASER SHOCK PROCESSING (LSP)	33
2.4.2.2	EFFECTS OF LASER PARAMETERS ON SURFACE TEXTURING	34
2.5	FRICITION AND WEAR TESTING	36
2.6	FRICITION AND WEAR OF TEXTURED STEELS	39
2.6.1	DRY CONDITION	39
2.6.2	LUBRICATED CONDITION	41
2.7	FORMULATION OF THE PROBLEM	45
Chapter 3	EXPERIMENTAL PROCEDURE	47
3.1	PROCUREMENT OF MATERIAL	48
3.2	DETERMINATION OF THE CHEMICAL COMPOSITION	48
3.3	SAMPLE PREPARATION	48
3.4	LASER SURFACE TEXTURING	49
3.5	CHARACTERIZATION OF DIMPLES	54
3.6	FRICITION AND WEAR TESTING	55
3.6.1	DRY CONDITION	55
3.6.2	LUBRICATED CONDITION	56
3.7	EXAMINATION OF WORN SURFACES	58
Chapter 4	TRIBOLOGICAL BEHAVIOUR OF TEXTURED DISC IN DRY CONDITION	59
4.1	RESULTS	60

4.1.1	CHEMICAL COMPOSITION OF AISI52100	60
4.1.2	CHARACTERIZATION OF LASER TEXTURED SURFACE	60
4.2	EFFECT OF LASER SURFACE TEXTURING ON THE FRICTION AND WEAR PROPERTIES	63
4.2.1	FRICTION BEHAVIOUR	63
4.2.2	WEAR BEHAVIOUR	71
4.3	EXAMINATION OF WORN SURFACE	73
4.4	DISCUSSION	83
Chapter 5	TRIBOLOGICAL BEHAVIOUR OF TEXTURED DISC IN LUBRICATED CONDITION	89
5.1	EFFECT OF LASER SURFACE TEXTURING ON THE FRICTION AND WEAR PROPERTIES	90
5.1.1	FRICTION BEHAVIOUR	90
5.1.2	WEAR BEHAVIOUR	106
5.1.3	WORN SURFACE MORPHOLOGY	113
5.2	LUBRICATION REGIMES	132
5.3	DISCUSSION	135
Chapter 6	CONCLUSIONS AND FUTURE WORK	147
6.1	CHARACTERIZATION AND FRICTION AND WEAR PERFORMANCE OF LASER TEXTURED BEARING STEEL UNDER DRY SLIDING	148
6.1.1	CHARACTERIZATION OF LASER TEXTURED BEARING STEEL	148
6.1.2	FRICTION AND WEAR BEHAVIOUR UNDER DRY SLIDING	148

6.1.3	FRICITION AND WEAR PERFORMANCE OF LASER TEXTURED BEARING STEEL UNDER LUBRICATED SLIDING	152
6.1.4	REGIMES OF LUBRICATION	154
6.2	FUTURE SCOPE	156
	<i>REFERENCES</i>	157
	<i>LIST OF PUBLICATIONS</i>	171

LIST OF FIGURES

Fig. 1.1	Graphical representation of the multidisciplinary notion of tribology in relation to other sciences.	3
Fig. 2.1	Schematic diagram of surface topography, various surface films and interaction at asperities.	11
Fig. 2.2	Mean film thickness in different lubrication regimes.	21
Fig. 2.3	Different lubrication regimes observed in fluid lubrication.	23
Fig. 2.4	The lubrication states and typical friction coefficients.	24
Fig. 2.5	Commonly used texture shapes with flat bottom profile (a) and curved bottom profile (b).	27
Fig. 2.6	The three types of surface texturing and six typical texture arrangements arising from directional dependency.	27
Fig. 2.7	Discs with different array of dimples: a) untextured, b) spiral array, c) radial array, d) random array, e) concentric array, f) square array.	30
Fig. 2.8	Schematics of laser processing using—(a) fs and ps laser (b) ns laser (c) ms; and (d) cw laser.	35
Fig. 2.9	The various components constituting a tribosystem.	37
Fig. 2.10	Schematic illustration of a pin-on-disc wear test.	39
Fig. 2.11	SEM images of laser textured 30 NiCrMo12 nitride steel (a); an individual dimple filled with the wear debris (b).	41
Fig. 2.12	Mechanism of pressure development: velocity distribution – parallel surfaces (a); velocity distribution – non – parallel surfaces (b).	42
Fig. 2.13	Schematic illustration of parallel sliding surfaces with a single dimple (a), and the hydrodynamic pressure distribution over the single dimple (b).	43

Fig. 2.14	(a) A partial laser surface textured parallel slider bearing cross-section. (b) The effect of the texturing on the load-bearing capacity.	44
Fig. 3.1	Schematic diagram of counterface pin (all dimensions in mm).	49
Fig. 3.2	Shapes of dimples used in the study	50
Fig. 3.3	Film thickness and geometry of micro-dimples.	50
Fig. 3.4	Cross-sectional profile of a single dimple	51
Fig. 3.5	CAD images of the discs textured with a spiral array of (a) circular dimples, density 7%, (b) circular dimples, density 20%, (c) bi-triangular, density 7%, and (d) bi-triangular, density 20%.	53
Fig. 4.1	Laser textured disc and a pin.	61
Fig. 4.2	Optical micrographs of laser textured surface of steel discs having (a) 7% density of circular dimples (CT7), (b) 20% density of circular dimples (CT20), (c) 7% density of bi-triangular dimples (BT7) and (d) 20% density of bi-triangular dimples (BT20).	62
Fig. 4.3	SEM micrograph (a, c) and 2D profile illustrating the lengths, average depth and height of micro-pores (b, d).	63
Fig. 4.4	Variation of friction coefficient with the number of revolutions at a speed of 0.2 m/s and 15 N load.	64
Fig. 4.5	Variation of friction coefficient with the number of revolutions at a speed of 0.6 m/s and 15 N load.	65
Fig. 4.6	Variation of friction coefficient with the number of revolutions at a speed of 1 m/s and 15 N load.	66
Fig. 4.7	Variation of friction coefficient with the number of revolutions at a speed of 0.2 m/s and 30 N load.	67
Fig. 4.8	Variation of friction coefficient with the number of	68

	revolutions at a speed of 0.6 m/s and 30 N load.	
Fig. 4.9	Variation of friction coefficient with the number of revolutions at a speed of 1 m/s and 30 N load.	69
Fig. 4.10	Average coefficient of friction for various samples at different speeds and 15 N load.	70
Fig. 4.11	Average coefficient of friction for various samples at different speeds and 30 N load.	71
Fig. 4.12	Variation of wear rate in textured specimens at different speeds under 15 N load.	72
Fig. 4.13	Variation of wear rate in textured specimens at different speeds under 30 N load.	73
Fig. 4.14	Scanning electron micrographs of worn surface of specimens after sliding under the dry condition at 15 N constant load at 0.2m/s.	74
Fig. 4.15	Scanning electron micrographs of worn surface of specimens after sliding under the dry condition at 15 N constant load at 0.6m/s.	75
Fig. 4.16	Scanning electron micrographs of worn surface of specimens after sliding under the dry condition at 15 N constant load at 1.0 m/s.	77
Fig. 4.17	Scanning electron micrographs of worn surface of specimens after sliding under the dry condition at 30 N constant load at 0.2 m/s.	78
Fig. 4.18	Scanning electron micrographs of worn surface of specimens after sliding under the dry condition at 30 N constant load at 0.6 m/s.	79
Fig. 4.19	Scanning electron micrographs of worn surface of specimens after sliding under the dry condition at 30 N	80

	constant load at 1.0 m/s.	
Fig. 4.20	SEM-EDS of worn surface of CT20 after sliding under dry condition at 15 N constant load at 1.0 m/s.	81
Fig. 4.21	SEM-EDS of worn surface of BT7 after sliding under dry condition at 30 N constant load at 0.6 m/s.	82
Fig. 4.22	Optical 3D Profilometry of disc surfaces before (a) and after (b) the test at 1 m/s speed and 15 N load.	83
Fig. 5.1	Variation of coefficient of friction with number of revolutions at different speeds and a constant load of 10 N for (a) UT, (b) CT7, (c) CT20, (d) BT7 and, (e) BT20	92
Fig. 5.2	Variation of coefficient of friction with the number of revolutions at different speeds and a constant load of 30 N for (a) UT, (b) CT7, (c) CT20, (d) BT7, and, (e) BT20	95
Fig. 5.3	Variation of coefficient of friction with number of revolutions at different speeds and a constant load of 50 N for (a) UT, (b) CT7, (c) CT20, (d) BT7 and, (e) BT20	98
Fig. 5.4	Average coefficient of friction for various samples at different speeds and at a constant load of 10 N	100
Fig. 5.5	Average coefficient of friction for various samples at different speeds and at a constant load of 30 N	101
Fig. 5.6	Average coefficient of friction for various samples at different speeds and at a constant load of 50 N	102
Fig. 5.7	Average coefficient of friction for various samples at different loads and at a speed of 0.2 m/s	103
Fig. 5.8	Average coefficient of friction for various samples at different loads and at a speed of 0.8 m/s	104
Fig. 5.9	Average coefficient of friction for various samples at different loads and at a speed of 1.4 m/s	105
Fig. 5.10	Average coefficient of friction for various samples at	106

	different loads and at a speed of 2 m/s	
Fig. 5.11	Variation of wear rate in textured specimens at different speeds under a load of 10 N	107
Fig. 5.12	Variation of wear rate in textured specimens at different speeds under a constant load of 30 N	108
Fig. 5.13	Variation of wear rate in textured specimens at different speeds under a constant load of 50 N	109
Fig. 5.14	Variation of wear rate in specimens at different loads at a constant speed of 0.2 m/s	110
Fig. 5.15	Variation of wear rate in specimens at different loads at a constant speed of 0.8 m/s	111
Fig. 5.16	Variation of wear rate in specimens at different loads at a constant speed of 1.4 m/s	112
Fig. 5.17	Variation of wear rate in specimens at different loads at a constant speed of 2.0 m/s	113
Fig. 5.18	Scanning electron micrographs of worn surface of UT under a load of 10 N load and at different speeds.	114
Fig. 5.19	Scanning electron micrographs of worn surface of CT7 under 10 N load and at different speeds.	115
Fig. 5.20	Scanning electron micrographs of worn surface of CT20 under 10 N load and at different speeds.	116
Fig. 5.21	Scanning electron micrographs of worn surface of BT7 under 10 N load and at different speeds.	117
Fig. 5.22	Scanning electron micrographs of worn surface of BT20 under 10 N load and at different speeds.	118
Fig. 5.23	Scanning electron micrographs of worn surface of UT under 30 N load and at different speeds.	119
Fig. 5.24	Scanning electron micrographs of worn surface of CT7 under 30 N load and at different speeds.	120

Fig. 5.25	Scanning electron micrographs of worn surface of CT20 under 30 N load and at different speeds.	121
Fig. 5.26	Scanning electron micrographs of worn surface of BT7 under 30 N load and at different speeds	122
Fig. 5.27	Scanning electron micrographs of worn surface of BT20 under 30 N load and at different speeds.	123
Fig. 5.28	Scanning electron micrographs of worn surface of UT under 50 N load and at different speeds.	124
Fig. 5.29	Scanning electron micrographs of worn surface of CT7 under 50 N load and at different speeds.	125
Fig. 5.30	Scanning electron micrographs of worn surface of CT20 under 50 N load and at different speeds.	126
Fig. 5.31	Scanning electron micrographs of worn surface of BT7 under 50 N load and at different speeds.	127
Fig. 5.32	Scanning electron micrographs of worn surface of BT20 under 50 N load and at different speeds.	128
Fig. 5.33	SEM-EDS of worn surface of BT7 at a constant load of 10 N and sped of 1.4 m/s	129
Fig. 5.34	Worn track and depth of a dimple (before and after the test) for BT7 tested at 0.8 m/s under 10N load	130
Fig. 5.35	3D Optical profilometry of BT7 slid at a load of 10 N at 0.2 m/s before (a) and after the test (b)	131
Fig. 5.36	Variation of coefficient of friction for CT20 for a maximum number of revolutions at different speeds and 10N load.	132
Fig. 5.37	Average coefficient of friction of discs at various sliding speeds, 10 N load in single drop lubrication.	133
Fig. 5.38	Average coefficient of friction of discs at various sliding speeds, 30 N load in single drop lubrication.	134

Fig. 5.39	Average coefficient of friction of discs at various sliding speeds, 50 N load in single drop lubrication.	135
Fig. 5.40	Schematic illustration depicting the plausible friction reduction mechanism under dry sliding condition	144
Fig. 5.41	Schematic illustration depicting the probable friction reduction mechanism under single drop lubrication	145

LIST OF TABLES

Table 3.1	Analytical description of cross-sectional profile for textures.	52
Table 3.2	Surface texturing parameters.	52
Table 3.3	Laser surface texturing parameters.	54
Table 3.4	Experimental conditions used for investigating the tribological performance under dry conditions.	56
Table 3.5	Experimental conditions used for investigating the tribological performance under lubricated conditions	57
Table 3.6	Physical properties of oil used for testing	57
Table 4.1	Chemical composition of bearing steel (wt. %).	60
Table 4.2	Sample designation and dimple features.	62

LIST OF ABBREVIATIONS/SYMBOLS

a_{dimple}	:	Area of a dimple
A_{disc}	:	Area of the disc
A_r	:	Real Area of Contact in plastic deformation
<i>ASTM</i>	:	American Society for Testing of Materials
B_p	:	Slider width
<i>BT20</i>	:	Bi-Triangular textured with 20% dimple density
<i>BT7</i>	:	Bi-Triangular textured with 7% dimple density
<i>CAD</i>	:	Computer-aided design
<i>COF</i>	:	Coefficient of friction
<i>CT20</i>	:	Circular textured with 20% dimple density
<i>CT7</i>	:	Circular textured with 7% dimple density
<i>CW</i>	:	Contineous wave
D	:	Diameter of the disc
d	:	Diameter of a circular dimple
<i>DLIP</i>	:	Direct laser interference patterning
<i>EDS</i>	:	Energy-dispersive X-ray spectroscopy
F_a	:	Force needed to shear adhered junctions
F_d	:	Force needed to supply the energy of deformation
<i>fs</i>	:	Femto-second
H	:	Hardness of the softer of the contacting materials
<i>HAZ</i>	:	Heat affected zone
h_{max}	:	Maximum clearance

h_p	:	Dimple depth
H_p	:	Dimensionless dimple depth
L	:	Total sliding distance
LSP	:	Laser shock processing
LST	:	Laser surface texturing
MPa	:	Mega Pascal
ms	:	Milli-second
ns	:	Nano-second
p	:	Mean yield stress of asperities of softer of the two materials
P_a	:	Ambient pressure
P_c	:	Cavitation pressure
ps	:	Pico-second
R_a	:	Roughness Average
r_p	:	Base radius
SEM	:	Scanning Electron Microscopy
S_p	:	Area density
U	:	Sliding speed
UT	:	Untextured
V	:	Total wear volume
WTD	:	Wear track diameter
μ	:	Coefficient of friction
μ_k	:	Kinetic friction
μ_s	:	Static friction
τ_a	:	The average shear strength

PREFACE

Friction, wear, and lubrication are three different aspects of tribology. Tribology is the study of surfaces moving relative to one another, and it influences our daily activities in a variety of ways. It has a very long history and is still more fascinating, making it both old and young. It has applications practically in every industry, including machine elements, manufacturing processes, automotive, space, renewable energy, and bio-tribology. The friction in mechanical systems wastes a significant amount of energy, and finding solutions to reduce friction and wear through the use of novel surfaces, materials, and lubrication technologies are critical for a greener and more sustainable future. Surface engineering incorporates chemical, structural, and morphological changes through material addition or modification of surface topography and can be used as an instrument to solve tribological problems.

Surface texturing is one of the approaches that is being used in reducing friction and wear in a wide spectrum of applications. It is the process of altering the topography of a surface to create uniform features with regularly formed cavities or protrusions. Laser Surface Texturing (LST) has been used to texture steel surfaces using regular arrays of micro-dimples because it has a short processing time, is environmentally friendly, does not require vacuum, and allows for excellent and easy control of the shape and size of the ablated micro-textures by tuning the characteristic of the laser spot. The textures require a precise design to provide favourable benefits, particularly in lubricated contact. Shape, size, depth, and arrangement on the surface are all textural characteristics that govern the tribological performance of mating bodies under different operating conditions. The textures act as a trap for wear debris under dry sliding contact, whereas these provide an increased load-bearing capacity to the moving surfaces under lubricated sliding. Therefore, developing cost-effective surface texturing methods for low-cost

component production and carefully selecting texture patterns for surface texturing to be useful are important obstacles for successful surface texturing in tribological applications.

The tribological performance of textured surfaces has been reported to be significantly affected by the morphology of textures like shape (circular, spherical, elliptical, triangular etc.), size and aspect ratio. Additionally, the array of dimples on the surface has also been reported to play a significant role in controlling friction. A spiral array has a more and stable number of micro-dimples than a radial array under the same contact area, so the density of dimples becomes essential. The operating parameters such as load, speed, and environmental conditions such as dry or lubricated contact, temperature, and humidity also play an important role in dictating friction and wear characteristics. Under low load and high-speed conditions, large/ shallow dimples (high aspect ratio) favour the hydrodynamic effect. Also, in full lubrication, the hydrodynamic effect is more pronounced; however, there are many instances where starved lubrication occurs.

In view of the above, it becomes imperative to explore the potential of surface texturing as an effective means for reducing both friction and wear of mating bodies having a different shape, density and array of textures at different load and speed conditions under both dry and lubricated conditions. The present work introduces a new bi-triangular shape of dimples arranged in a spiral array, and the study has been carried out in parts; (i) friction and wear performance of laser textured bearing steel under dry sliding and (ii) friction and wear performance of laser textured bearing steel under lubricated sliding with a “single drop lubrication”. The surface texturing of bearing steel has been performed to create bi-triangular dimples along with circular dimples with two different densities. The untextured and textured surfaces having circular dimples have

been used for a comparative study with the bi-triangular dimples. The friction and wear characteristics have been examined using a pin-on-disc test rig with untextured/textured disc as a rotating specimen against a stationary flat pin providing a conformal contact. The single drop lubrication is employed using low load and low to high-speed conditions under conformal contact on an open system by using fresh oil on each new sliding track.

The present thesis has been organised into six chapters, as summarised below:

Chapter 1 includes the introductory remarks emphasising the technological importance of the problem under consideration.

Chapter 2 begins with a critical review of the existing literature on surface interactions and their repercussions, such as friction and surface wear. It is followed by a brief narrative on various strategies for reducing friction and wear, with a focus on surface texture. A brief description of the many types of lubricants (liquid, semi-solid, solid, and gaseous) has also been included, along with a detailed description of the lubrication regimes that arise in various operating conditions. Some typical friction coefficients corresponding to the lubrication states are also mentioned, which have been used in the present work. Three operating regimes based on load and speed ranges have been described, and these have been utilised to select load and speed for the current investigation. The chapter goes on to discuss the effect of surface features such as shape, size, aspect ratio, array and directionality on friction and wear performance. This is followed by a detailed analysis of the literature on laser surface texturing, types, and parameters that affect laser ablation. The chapter also includes a critical presentation of the existing literature emphasising the role of laser surface texturing in enhancing the tribological performance of a system. The formulation of the problem is presented at the end of the chapter.

Chapter 3 outlines the details of materials and experimental procedures used in the present study to explore the tribological performance of textured specimens. In the

current investigation, circular disc-shaped (ϕ 50 mm \times 5 mm) specimens and pin as a counter specimen of bearing steel (AISI52100), have been used. The disc has been laser textured with bi-triangular and circular dimples having 7 % and 20 % density at Laser Job Works, Noida, India. The non-contact optical profilometry and SEM have been used for the characterization of textured specimens. The friction and wear characteristics have been examined under unidirectional sliding using a pin-on-disc set up under dry contact condition at sliding speeds of 0.2 m/s, 0.6 m/s and 1 m/s under the applied normal loads of 15 N and 30 N. However, under single drop lubrication, the sliding speeds of 0.2 m/s, 0.8 m/s, 1.4 m/s and 2 m/s have been used under normal loads of 10 N, 30 N and 50 N. In both conditions, tribological performance of bearing steel has been investigated for shorter (8000 cycles) and as well as tested for durability check for a longer duration (20000). The details of techniques such as optical microscopy, scanning electron microscopy (SEM) equipped with energy dispersive spectroscopy (EDS), and non-contact optical profilometry used to characterise the worn surfaces have also been included in this chapter.

Chapter 4 is devoted to the friction and wear behaviour of textured steels under dry sliding contact and begins with the results on the characterization of bearing steel and surface texturing. The size of each dimple is \sim 500 μ m with an average depth of 8 μ m, as revealed by non-contact optical profilometry. The distance between consecutive dimples in an array is measured as 1599.67 μ m for 7% density of circular dimples, and for 20% density of dimples, the distance decreases to \sim 700 μ m. Untextured samples are designated as UT, while textured samples with bi-triangular dimples and circular dimples are designated as BT7, BT20, and CT7, CT20, respectively, with 7 and 20 indicating dimple density. The SEM micrograph revealed the presence of typical bulges at the brim of the dimple due to the deposition of metal during ablation.

The chapter also contains the results and discussion pertaining to the friction and wear behaviour of the specimens at the loads of 15 and 30 N and speeds of 0.2, 0.6 and 1.0 m/s under unidirectional sliding in dry conditions. The friction coefficient shown by UT at 0.6 m/s under 15 N load is the highest (~ 0.68), whereas that shown by BT20 at 0.6 m/s under 30 N load is the lowest (~ 0.51).

The average coefficient of friction for UT, CT7, CT20, BT7, BT20 at different sliding speeds and a constant load of 15 N has been found to be the highest at 0.6 m/s and the lowest at 0.2 m/s, with the exception of untextured (UT) and BT20. At 1.0 m/s, the coefficient of friction has been observed to fall in between. At the lowest speed of 0.2 m/s used in the present investigation, the coefficient of friction is found to decrease after texturing with 7% density circular dimples and remained in the same band for CT20 and BT7 before increasing finally for BT20. A similar trend of variation has been observed for a speed of 0.6 m/s, except that a decrease in coefficient of friction is observed from BT7 to BT20. However, at the highest speed of 1.0 m/s, the coefficient of friction is found to increase as one moves from untextured to CT7 before decreasing continuously as one moves from CT7 to CT20 to BT7 to BT20, indicating thus, the effect of density as well as the shape on friction reduction. At a load of 30 N, the average coefficient of friction is the highest at 0.2 m/s and the lowest at 1.0 m/s for all the specimens with the exception of BT20. At the lowest speed of 0.2 m/s, the coefficient of friction is observed to decrease after texturing with 20% density circular and bi-triangular dimples and remained in the same band for BT7 and CT7. A similar trend of variation has been observed for a speed of 0.6 m/s and at the highest speed of 1.0 m/s.

As far as the wear rate is concerned, textured specimens have shown a lower wear rate than the untextured sample at all the speeds used in the present study. The wear rate has been observed to either decrease or remains constant as one moves from CT7 to

BT7 at speeds of 0.2 and 1.0 m/s, whereas it is found to increase from CT20 to BT7 at a speed of 0.6 m/s. The wear rate is found to decrease from BT7 to BT20 as the speed changes from 0.6 and 1.0 m/s, whereas an increase has been observed for a speed of 0.2 m/s. A relatively more wear in the 7% circle density disc (CT7) has been attributed to the hard deposition on the surface surrounding the cavities. A higher wear of textured disc with 20% bi-triangular dimples density (BT20) at 0.2 m/s has been ascribed to initial presence of deposited material and its subsequent wear. At a constant load of 30 N and a speed of 0.2 m/s, the wear rate is found to decrease from UT to CT20 and remained almost constant till BT7 before increasing for BT20. However, the wear rate is observed to decrease as one moves from UT to BT7, followed by a slight increase thereafter for BT20 at sliding speeds of 0.6 and 1.0 m/s.

The observed friction and wear behaviour for the untextured steel has been explained on the basis of the adhesion between disk and counterface pin followed by the generation of wear debris due to relative motion. The debris either gets trapped between the sliding surfaces or may get ejected from the interface due to centrifugal forces. The debris trapped between the surface may form a compacted transfer layer on the sliding surface and result in a reduction in both friction and wear, if that gets oxidized during continued rubbing, by providing low-shear strength junctions at the interface and protecting the underlying surface from direct metal to metal contact. As far as textured steels are concerned, the behaviour has been explained on the basis presence and removal of bulges at the brim dimples, the capability of the dimples to trap the wear debris particles, the extent of filling of dimples, the presence of loose debris particles, and the formation of the transfer layer and its extent of compaction depending upon the conditions load and speed.

In the end, the results have been discussed to have a coherent understanding of the role of textures in affecting the friction and wear between the tribo-pair.

Chapter 5 includes the results of the unidirectional sliding test in single drop lubrication. The results on tribological behaviour under sliding are presented for untextured, textured specimens at all loads and speeds.

At a load of 10N, the coefficient of friction for UT is observed to increase with increasing speed from 0.2 to 1.4 m/s, followed by a decrease thereafter and the value varies from 0.22 to 0.28. However, bi-triangular dimples, i.e., BT7 and BT20 have shown an increase in the average coefficient of friction with increasing speed from 0.2 m/s to 2.0 m/s. In contrast, the average coefficient of friction is found to decrease sharply for specimens having circular dimples i.e., CT7 & CT20, as the speed is raised from 0.2 m/s to 1.4 m/s followed by an increase for the speed of 2.0 m/s. The average coefficient of friction at any speed is also found to be relatively lower for a lesser fraction of area coverage by the dimples, i.e., for BT7 and CT7, and higher for an increased fraction of area coverage (BT20 and CT20) which highlights the effect of dimple density on the frictional performance. At a particular speed (say 0.2 m/s), the average coefficient of friction observed for the sample having 7% density with bi-triangular shape (BT7) is the lowest and that for the sample having 20% density with circular dimples (CT20) is the highest. The value of the coefficient of friction for CT7 and BT20 falls in-between, with CT7 having a lower coefficient of friction than BT20, reflecting, thus, the combined effect of density and shape of the dimples on friction reduction. A similar pattern of variation is also observed at the other speeds.

The coefficient of friction for UT is observed to decrease with increasing speed from 0.2 to 1.4 m/s, followed by an increase thereafter and the value varies from 0.21 to

0.22 for a load of 30 N. BT20 has shown an increase in the average coefficient of friction with increasing speed from 0.2 m/s to 0.8 m/s followed by a decrease at 1.4 m/s before increasing at 2 m/s for BT20. The coefficient of friction CT7 has been observed to increase from 0.2 m/s to 0.8 m/s; however, a decrease in the value for CT20 is observed for this speed range. The average coefficient of friction for CT7 falls as speed increases from 0.8 to 2 m/s, whereas it is found to remain almost constant for CT20 in this speed range. An increase in the average coefficient of friction for both BT20 and CT20 has been observed with increasing speed from 0.8 m/s to 2 m/s. Both BT7 and BT20 show a similar trend for all the speeds with almost the same values of the average coefficient of friction. At a load of 50N, the average coefficient of friction for the untextured sample as well as CT7 has been found to decrease with an increase in speed from 0.2 to 2 m/s, whereas the same for BT20 is observed to increase with increasing speed from 0.2 to 1.4 m/s followed by a marginal decrease till 2.0 m/s. The average coefficient of friction for CT20 and BT7 has been found to decrease continuously with increasing speed. The average coefficient of friction by BT7 is consistently lower than other specimens at all speeds except at 0.2 m/s, where BT20 has a slightly lower coefficient of friction.

The wear rate for UT, CT7, CT20, BT7, and BT20 under different loads of 10, 30 and 50 N and at a constant speed of 0.2 m/s is found to decrease from 10 to 30 N followed by an increase thereafter for 50 N for all the specimens. However, the rate of decrease from 10 to 30 N is relatively sharp for CT20 and BT20 in comparison to UT and CT7. As far as an increase in wear rate from 30 to 50 N is concerned, the increase is relatively sharp for CT7 and CT20, whereas it is almost the same for UT and BT20. For all the loads, the UT specimen has shown the highest wear rate and BT7 the lowest. At loads of 10 and 30 N, CT20 and BT20 have a higher wear rate than CT7 and BT7. The

specimen with 7 % circular dimples, i.e., CT7 has the highest wear rate among all the textured samples at the highest load of 50 N used in the present study.

The wear rate for untextured specimens, i.e., UT is observed to decrease from 10 to 30 N, followed by an increase for 50 N, and it has shown the highest wear rate at all the loads at a constant speed of 0.8 m/s. The wear rate for CT7 is found to increase as the load is increased from 10 to 50 N with a sharp rise from 30 to 50 N, whereas CT20 has shown a continuously decreasing trend with an increasing load from 10 to 50 N. The wear rate for BT7 is almost found to be the same at 10 and 30 N, whereas it is observed to decrease beyond 30 N. The wear rate for BT20 is observed to increase as the load is raised from 10 to 30 N which is followed by a decrease for 50 N. However, BT7 has shown the lowest wear at all the loads at a speed of 0.8 m/s. At a constant speed of 1.4 m/s, the wear rate for UT, CT7, CT20, and BT7 has been observed to increase with increasing load from 10 to 50 N, whereas for BT20, it is found to decrease as the load is raised from 10 to 30 N followed by an increase to 50 N. UT has the highest wear rate at all the loads, whereas BT7 has the lowest except at 10 N load, for which CT7 has shown the lowest wear rate. The wear rate for UT, CT7, and BT7 has been observed to increase with increasing load from 10 to 50 N at a constant speed of 2.0 m/s, whereas for CT20 and BT20, it decreases from 10 to 30 N, followed by an increase thereafter for 50 N. CT20 and BT20 have shown relatively higher wear rate at the lowest load of 10 N, whereas at loads of 30 and 50 N, UT has the highest wear rate. The observed friction and wear behaviour has been explained on the basis of the presence of micro-bearings during the test and gradual filling of dimples by worn particles with increasing speed depending on load and speed and density of dimples, complete filling of dimples by wear debris, depletion of lubricant due to its limited supply disappearance of dimples and the micro-bearing effect.

Both lower density as well as bi-triangular shape, showed a better performance in comparison to a circular one. Different lubrication regimes, namely, boundary, mixed, and EHL depending on the shape, the density of dimples, and speed, were observed with CT7 and CT20 showing the boundary and mixed lubrication regime under all the speeds used in the study. However, BT7 showed a regime of mixed lubrication at lower speed which changed to EHL at higher speeds, whereas BT20 remained under boundary lubrication regime for the speeds. The coefficient of friction and wear rate did not vary monotonically with the density of dimples. Due to surface texturing, the friction force was reduced for a textured surface by around 69% for BT7 compared to the untextured sample. The friction coefficient has been found to reduce by about 35% by surface texturing with a density of 7% as compared with 20% density of the dimples for BT7. The bi-triangular texture with a density of 7% showed the optimum performance in terms of reduced friction and wear rate under the conditions of sliding used in the present study.

Chapter 6 presents the major conclusions of the present study pertaining to (i) friction and wear performance of laser textured bearing steel under dry sliding, (ii) friction and wear performance of laser textured bearing steel under lubricated sliding, along with the future scope of the work.